

## Hysteresis effects in the phase diagram of multiferroic $\text{GdMnO}_3$

J. Baier,<sup>1</sup> D. Meier,<sup>1</sup> K. Berggold,<sup>1</sup> J. Hemberger,<sup>2</sup> A. Balbashov,<sup>3</sup> J. A. Mydosh,<sup>1</sup> and T. Lorenz<sup>1,\*</sup>

<sup>1</sup>*II. Physikalisches Institut, University of Cologne, 50937 Cologne, Germany*

<sup>2</sup>*Experimentalphysik V, Institut für Physik, University of Augsburg, 86135 Augsburg, Germany*

<sup>3</sup>*Moscow Power Engineering Institute, 105835 Moscow, Russia*

(Received 9 January 2006; published 6 March 2006)

We present high-resolution thermal expansion  $\alpha(T)$  and magnetostriction  $\Delta L(H)/L$  measurements of  $\text{GdMnO}_3$ , which develops an incommensurate antiferromagnetic order (ICAFM) below  $T_N \approx 42$  K and transforms into a canted A-type antiferromagnet (cAFM) below  $T_c \approx 20$  K. In addition, a ferroelectric polarization  $\mathbf{P} \parallel a$  is observed below  $T_{FE}$  for finite magnetic fields applied along the  $b$  direction. In zero-magnetic field, we find a strongly anisotropic thermal expansion with certain, rather broad anomalous features. In finite magnetic fields, however, very strong anomalies arise at  $T_c$  for fields applied along each of the orthorhombic axes and at  $T_{FE}$  for fields along the  $b$  axis. Both phase transitions are of first-order type and strongly hysteretic. We observe a downbending of the ICAFM-to-cAFM phase boundary  $T_c(H)$  for low magnetic fields and our data give evidence for coexisting phases in the low-field low-temperature range.

DOI: [10.1103/PhysRevB.73.100402](https://doi.org/10.1103/PhysRevB.73.100402)

PACS number(s): 75.47.Lx, 64.70.Rh, 65.40.De, 75.80.+q

The recent discovery of very large magnetoelectric effects in the rare-earth manganites  $\text{RMnO}_3$  has reopened the field of the so-called multiferroic materials.<sup>1,2</sup> Multiferroic means, that several ferro-type orders, such as ferromagnetism, ferroelectricity or ferroelasticity coexist. The rare-earth manganites  $\text{RMnO}_3$  may be grouped into the hexagonal ones ( $R = \text{Ho}, \dots, \text{Lu}$ ) and those with orthorhombically distorted perovskite structures ( $R = \text{La}, \dots, \text{Dy}$ ). The hexagonal  $\text{RMnO}_3$  show both, ferroelectric and magnetic order, but the respective ordering temperatures differ by an order of magnitude,  $T_{FE} \approx 1000$  K and  $T_N \approx 100$  K.<sup>3</sup> In contrast,  $\text{RMnO}_3$  with  $R = \text{Gd}, \text{Tb}$ , and  $\text{Dy}$  possess comparable transition temperatures for the magnetic and the ferroelectric ordering.<sup>1,2</sup> Both,  $\text{TbMnO}_3$  and  $\text{DyMnO}_3$  develop an incommensurate antiferromagnetic order (ICAFM) below about 40 K. The incommensurability continuously changes upon cooling and becomes almost constant below  $T_c \approx 28$  K and  $\approx 19$  K for  $R = \text{Tb}$  and  $\text{Dy}$ , respectively. The transition to this long-wavelength incommensurate antiferromagnetic (LT-ICAFM) phase is accompanied by ferroelectric (FE) ordering with a polarization  $\mathbf{P} \parallel c$ , which flops to  $\mathbf{P} \parallel a$  above a critical magnetic field applied along the  $a$  or  $b$  direction, while it is suppressed for large fields along  $c$ .<sup>4</sup>  $\text{GdMnO}_3$  also shows an ICAFM order below  $T_N \approx 42$  K and a second transition at  $T_c \approx 23$  K. Based on the observed weak ferromagnetism<sup>5,6</sup> and on x-ray diffraction studies<sup>7</sup> a canted A-type antiferromagnetic ordering (cAFM) has been proposed for  $T < T_c$ , but a direct magnetic structure determination has not yet been published. Both transition temperatures weakly increase in a magnetic field.<sup>4</sup> Concerning the FE polarization, contradictory results have been reported. Kuwahara *et al.*<sup>8,9</sup> find a finite polarization below 13 K, while Kimura *et al.*<sup>4</sup> observe FE order only between 5 K and 8 K. The magnitude of  $\mathbf{P}$  is much smaller than in  $\text{TbMnO}_3$  and  $\text{DyMnO}_3$  and the direction is  $\mathbf{P} \parallel a$ . Moreover, there are no magnetic-field-induced polarization flops. Instead the polarization is stabilized by a magnetic field along  $b$ , while it is immediately suppressed for fields along  $a$  and  $c$ .<sup>4,8,9</sup>

In order to study the coupling of the various phase boundaries to lattice degrees of freedom, we have conducted high-resolution measurements of thermal expansion and magnetostriction on  $\text{GdMnO}_3$ . We find pronounced anomalies at all transitions, i.e., all transitions strongly couple to the lattice. Thus, our data allow for a precise determination of the magnetic-field temperature phase diagram and clearly reveal that the ICAFM-to-cAFM as well as the FE transition are of first order with strong hysteresis. For low magnetic fields, we find a downbending of the ICAFM-to-cAFM phase boundary and evidence for a coexistence of both phases in this low-field range. This should be taken into account for further experiments, in particular for zero magnetic field. Probably, this may also explain the contradictory results reported for  $\text{GdMnO}_3$ .<sup>4,8-10</sup>

The  $\text{GdMnO}_3$  single crystal used in this study is a cuboid of dimensions  $1.7 \times 2 \times 1.45$  mm<sup>3</sup> along the  $a$ ,  $b$ , and  $c$  direction (Pbnm setting), respectively. It was cut from a larger crystal grown by floating-zone melting. Phase purity was checked by x-ray powder diffraction.<sup>11</sup> Magnetization, resistivity, and specific heat data of the same crystal are reported in Ref. 6. The linear thermal expansion  $\alpha_i = \partial \ln L_i / \partial T$  and magnetostriction  $\Delta L_i(H)/L_i = [L_i(H) - L_i(0)]/L_i(0)$  have been measured by a home-built high-resolution capacitance dilatometer.<sup>12</sup> Here,  $L_i$  denote the lengths parallel to the different crystal axes  $i = a, b$ , and  $c$ . In general, we studied the length changes in longitudinal magnetic fields up to 14 T, i.e.,  $H \parallel i$ , and, in addition, we measured  $\alpha_b$  for  $H \parallel c$ .

Figure 1 shows the zero-field  $\alpha_i$  of  $\text{GdMnO}_3$  for  $i = a, b$ , and  $c$ , which are strongly anisotropic and show several anomalies. The sharp anomalies around 42 K signal the Néel transition of the Mn ions and their shape is typical for a second-order phase transition. According to previous publications further anomalies are expected at lower  $T$ : (i) At the ICAFM-to-cAFM transition around  $T_c \approx 23$  K, (ii) around  $T_{FE} \approx 10$  K, where the FE ordering sets in, and (iii) around 6 K due to the ordering of the Gd moments. Indeed, there are pronounced anomalies around 6 K, small ones around 10 K,

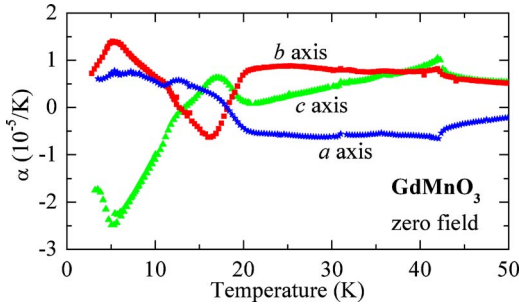


FIG. 1. (Color online) Thermal expansion of  $\text{GdMnO}_3$  along  $a$ ,  $b$ , and  $c$ .

and intermediate ones around 20 K with different signs and magnitudes for the different  $i$ . However, all these anomalies are rather broad making a clear identification of transition temperatures difficult. This drastically changes for finite magnetic fields.

In Fig. 2, we show  $\alpha_a(T)$  for  $H \parallel a$ . With increasing magnetic field, a broad anomaly shows up around 10 K, changes sign and smears out above 2 T. The origin of this anomaly is unclear, it may be related to the complex interplay of the magnetism of the Mn and Gd ions.<sup>6</sup> The most drastic change occurs, however, around 18 K, where a huge anomaly emerges between 0 and 1 T. This anomaly is close to the observed ICAFM-to-cAFM transition at  $T_c$  and systematically shifts to higher  $T$  with further increasing field, in agreement with the observed field dependence  $T_c(H)$ .<sup>1,4,7</sup> The negative sign of the anomaly means that the transition from the cAFM to the ICAFM phase, with increasing  $T$ , is accompanied by a pronounced contraction of the  $a$  axis (see also Fig. 3). The  $\alpha_a(T)$  curves of Fig. 2(a) have been recorded with increasing  $T$  in the so-called field-cooled (FC) mode, i.e., the field has been applied at  $T \approx 50$  K. We have also recorded the data during the cooling runs. Figure 2(b) compares  $\alpha_a(T)$  obtained with increasing and decreasing  $T$  for  $H=4$  T. Obviously, there is a strong hysteresis at the ICAFM-to-cAFM transition identifying this transition as first-order type.

The lower panels of Fig. 2 present the magnetostriction  $\Delta L_a(H)/L_a$  for  $H \parallel a$  at constant  $T$ . At 20 K, an anomalous expansion of the  $a$  axis occurs around 4 T, which is related to a transition from the ICAFM to the cAFM phase as a function of increasing  $H$ . Both, the position of the  $\Delta L_a(H)/L_a$  anomaly in the  $H$ - $T$  plane and its magnitude fit to the position and magnitude of the corresponding  $\alpha_a(T)$  anomaly due to the ICAFM-to-cAFM transition as a function of decreasing  $T$ . The  $\Delta L_a(H)/L_a$  curves obtained with increasing and decreasing  $H$  also show a hysteresis at the ICAFM-to-cAFM transition. With decreasing  $T$  the anomaly of  $\Delta L_a(H)/L_a$  shifts toward lower field. Around 12 K an anomalous expansion of the  $a$  axis is observed with increasing  $H$ , however, this expansion is not reversed upon decreasing the field. Due to the large hysteresis  $\text{GdMnO}_3$  remains in the cAFM phase after the magnetic field is switched off. With further decreasing  $T$ , the anomaly of  $\Delta L_a(H)/L_a$  again shifts to higher field and at 5 K the anomalous expansion occurring with increasing  $H$  is reversed again with decreasing

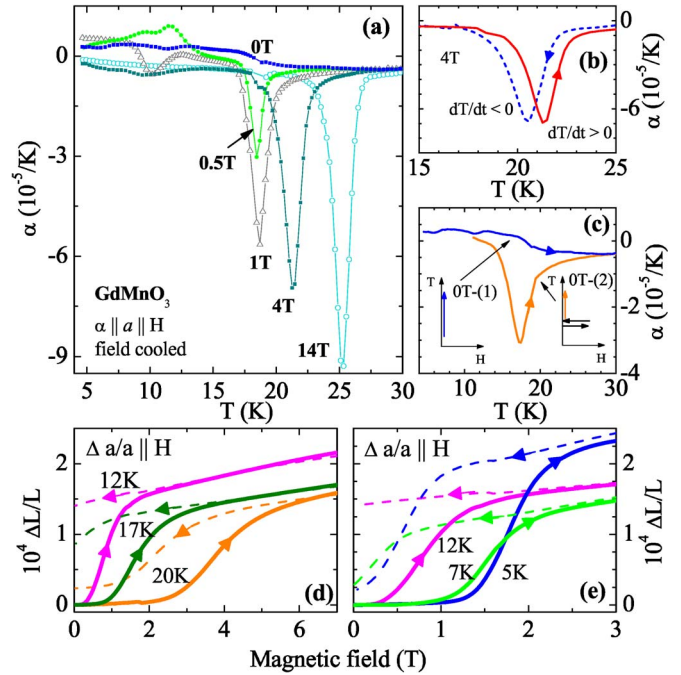


FIG. 2. (Color online) Panel (a): Field-cooled thermal expansion  $\alpha_a(T)$  for  $H \parallel a$  measured with increasing  $T$ . Panel (b) shows the hysteresis around  $T_c$  between the data obtained with increasing and decreasing  $T$ . Panel (c) compares two zero-field  $\alpha_a(T)$  curves for increasing  $T$ . The first curve [0T-(1)] has been recorded after zero-field cooling the sample and the second [0T-(2)] after cooling the sample to 12 K and subsequently applying and removing a magnetic field of 8 T. The lower panels (d) and (e) present the ZFC magnetostriction  $\Delta L_i(H)/L_i$  recorded with increasing (solid lines) and decreasing (dashed) field.

ing field. Apparently, we have traced the field-induced transition to the cAFM phase down to our lowest  $T$ . This means that the ICAFM-to-cAFM phase boundary  $T_c(H)$  shows a clear downbending in the low-field range (see Fig. 5). In order to verify this, we have carried out the following zero-field  $\alpha_a(T)$  measurement: after cooling the sample to 12 K in zero field, we have applied a magnetic field of 8 T in order to enter the cAFM phase and due to the hysteresis of the ICAFM-to-cAFM transition the sample should remain in the cAFM phase after removing the field again. Figure 2(c) shows a comparison of this zero-field  $\alpha_a(T)$  [labeled as 0T-(2)] with the conventional zero-field  $\alpha_a(T)$  [0T-(1)]. In contrast to the 0T-(1) curve, the 0T-(2) measurement shows a sharp peak around  $T_c$ , which is comparable to the anomaly of the finite-field  $\alpha_a(T)$  curves. This clearly confirms the downbending of the ICAFM-to-cAFM phase boundary. Thus, the (pure) cAFM phase of  $\text{GdMnO}_3$  cannot be reached by cooling the crystal in zero field. The broad anomalies in the zero-field  $\alpha_i(T)$  curves (see Fig. 1) probably arise from a partial ICAFM-to-cAFM transition and suggest that both phases coexist in the low-field region.

In Fig. 3, we compare the relative length changes as a function of field and temperature for all three axes. The  $c$  axis behaves similar to the  $a$  axis. The anomalies of  $c$  have the same signs but smaller magnitudes as compared to those of  $a$  and, moreover, their position for the same field (tem-

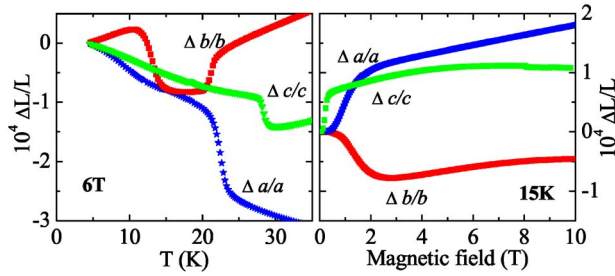


FIG. 3. (Color online) The relative length changes of the  $a$ ,  $b$ , and  $c$  axes as a function of  $T$  at constant field ( $H=6$  T; left) and as a function of  $H$  at constant temperature ( $T=15$  K; right). In all cases,  $H$  was applied parallel to the measured direction.

perature) is located at higher  $T$  (lower  $H$ ). Since in all cases we applied  $H\parallel L_i$ , the latter difference signals the anisotropy with respect to the field direction. Our results (not shown) for  $\alpha_c(T)$  and  $\Delta L_c(H)/L_c$  for other fields and temperatures, respectively, are very similar to those obtained for the  $a$  axis. In particular, the distinct expansion at the ICAFM-to-cAFM transition as a function of field or temperature is only present for  $H\geq 0.2$  T. The hysteresis is also strong for  $H\parallel c$ , but less pronounced than for  $H\parallel a$  (see Fig. 5). A different phenomenology is observed for  $\Delta L_b/L_b$  for  $H\parallel b$ . First, the anomalies at the ICAFM-to-cAFM transition are of opposite signs and, second, an additional anomaly occurs at a lower temperature.

In Fig. 4, we present  $\alpha_b(T)$  for different  $H\parallel b$ . Again, a very pronounced anomaly evolves around  $T_c\approx 18$  K in small fields and shifts to higher  $T$  with further increasing field. The behavior of  $\alpha_b$  is analogous to our results on  $\alpha_a$  and  $\alpha_c$ , however, an additional, very pronounced anomaly develops around 12 K in finite fields. Based on the polarization data of Ref. 4, we attribute this anomaly to the FE ordering at  $T_{FE}$ . As a further verification we have also measured  $\alpha_b$  in a transverse magnetic field  $H\parallel c$  and did not find such an additional anomaly [see inset of Fig. 4(a)]. As shown in the lower inset of Fig. 4(b), the transition to the FE phase is also of first-order type with a broad hysteresis. With further increase of the magnetic field above 8 T the magnitude of the  $T_{FE}$  anomaly decreases again and vanishes around 12 T. This disappearance is a consequence of the strong hysteresis of the FE transition and occurs only in the FC measurements of  $\alpha_b$ . The upper inset of Fig. 4(b) compares the FC and zero-field-cooled (ZFC) measurements of  $\alpha_b$  for  $H=12$  T  $\parallel b$ . The ZFC curve displays a large anomaly at  $T_{FE}$ , which is absent in the FC curve. This difference arises from a decreasing  $T_{FE}(H)$  with increasing field. When the lower  $T_{FE}(H)$  is smaller than our lowest measurement temperature of  $\approx 4.5$  K the FE phase cannot be reached in a FC run and, consequently, there is no anomaly in the subsequent  $\alpha_b(T)$  measured with increasing  $T$ . The FE phase can, however, be entered by cooling the sample in a lower field, e.g., 6 T [see lower inset of Fig. 4(b)] or in a ZFC run when the field is applied at the lowest temperature. Due to the large hysteresis, the sample remains in the FE phase up to high fields and therefore the ZFC  $\alpha_b(T)$  curves show anomalies at the upper  $T_{FE}(H)$  when the FE phase is left upon heating.

The lower panels (c) and (d) of Fig. 4 show the magne-

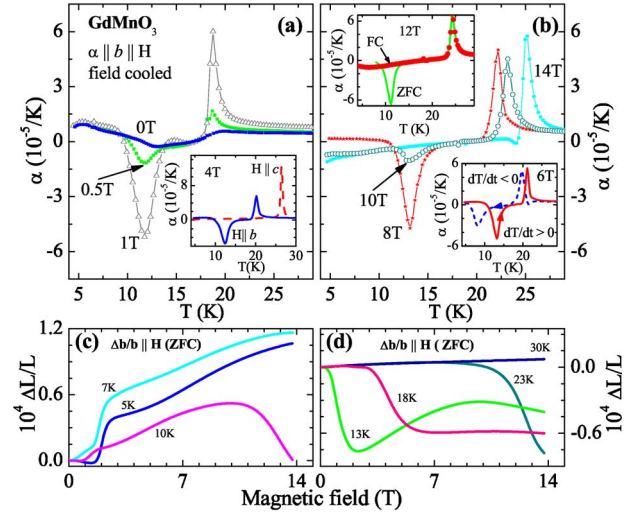


FIG. 4. (Color online) FC measurements of  $\alpha_b(T)$  in fields up to 1 T (a) and between 8 T and 14 T (b). The inset of panel (a) compares  $\alpha_b(T)$  for  $H=4$  T applied along  $b$  (solid line) and  $c$  (dashed). The upper inset of panel (b) shows  $\alpha_b(T)$  for  $H=12$  T ( $H\parallel b$ ;  $dT/dt>0$ ) obtained in a FC (symbols) and a ZFC run (line). The lower inset displays the hysteresis between  $\alpha_b(T)$  for  $H=6$  T recorded with  $dT/dt>0$  (solid line) and  $dT/dt<0$  (dashed). Panels (c) and (d) show the ZFC magnetostriction obtained for  $dH/dt>0$ .

tostriction. In agreement with the negative signs of the  $\alpha_b$  anomalies, we observe a pronounced contraction at the field-induced ICAFM-to-cAFM transition for  $T\geq 13$  K. At lower  $T$ , we still find clear anomalies, however, of opposite sign. This sign change results from the fact that below about 10 K the FE phase is entered, which has a significantly longer  $b$  axis than both, the cAFM phase and a low- $T$  extrapolation of the ICAFM phase (see Fig. 3). The strong decrease of  $\Delta b/b$  at 10 K for  $H\geq 10$  T signals a field-induced FE-to-cAFM transition due to the above-mentioned negative slope of the  $T_{FE}(H)$  boundary.

Based on our measurements of  $\alpha_i$  and  $\Delta L_i(H)/L_i$  with  $H\parallel i$  for all three crystallographic axes  $i$ , we derive the phase diagrams presented in Fig. 5. The weak field dependence of  $T_N\approx 42$  K well agrees with previous results.<sup>4</sup> The new feature of our phase diagram is the downbending of the ICAFM-to-cAFM phase boundary at low magnetic field. This transition exhibits a strong hysteresis and we conclude that the ICAFM and the cAFM phases coexist in the low-field low-temperature region. Such a coexistence can naturally explain why the zero-field  $\alpha_i(T)$  curves only show some broad anomalous features around 18 K instead of the distinct anomalies which signal the transition from the cAFM to the ICAFM phase for larger fields. This conclusion is also supported by measurements of the polarization showing that the magnitude of  $\mathbf{P}$  in this hysteretic region is much smaller than both,  $\mathbf{P}$  for larger  $H\parallel b$  and  $\mathbf{P}$  of  $\text{RMnO}_3$  with  $R=\text{Tb}$  and  $\text{Dy}$ .<sup>4</sup>

As shown in Fig. 4(a), the magnitudes of the  $\alpha_b$  anomalies at  $T_{FE}$  and  $T_c$  simultaneously evolve between 0 and 1 T. This correlation suggests that the ICAFM-to-cAFM transition is a precondition for the FE ordering. As mentioned above, the notation “cAFM” should be treated with some caution, because the magnetic structure of  $\text{GdMnO}_3$  has not yet been

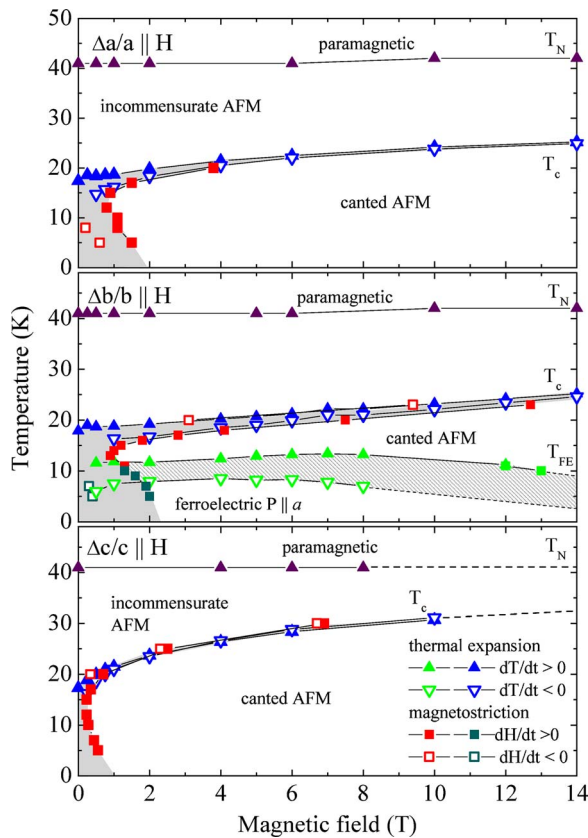


FIG. 5. (Color online) Phase diagrams of  $\text{GdMnO}_3$  based on the measurements of  $\alpha_i$  (triangles) and  $\Delta L_i(H)/L_i$  (squares) measured along  $i=a, b$ , and  $c$  with  $H||i$ . Filled and open symbols are obtained with increasing and decreasing  $T$  or  $H$ , respectively. Hatched areas signal regions of strong hysteresis, where different phases coexist.

unambiguously determined. In a simplified picture, the proposed structure can be described as follows: The Mn moments are oriented approximately along  $b$  with some canting toward  $c$ , along the  $a$  ( $c$ ) direction neighboring moments are essentially parallel (antiparallel) with respect to each other,

and along  $b$  an incommensurate modulation of the moments is present above and vanishes below  $T_c$ . This view is supported by the phase diagram, since the stabilization of the cAFM phase is most pronounced for  $H||c$  as it is expected for a cAFM phase with a weak ferromagnetic moment pointing along  $c$  already in zero field. A field along  $a$  also points approximately perpendicular to the Mn moments, and one can therefore expect that the Mn moments (and also the weak ferromagnetic moment) are slightly canted toward  $a$ . However, a more drastic change is expected for  $H||b$ , since 50% of the Mn moments are oriented roughly antiparallel to  $H$ . In simple antiferromagnets, this configuration usually leads to a spin-flop transition, i.e., the Mn moment would jump to the  $ac$  plane and cant towards  $b$ . Such a configuration would be analogous to those for  $H||a$  or  $c$  and according to Ref. 13 none of these configurations would lead to a finite polarization via a coupling of the magnetic and ferroelectric order parameters. However, in view of the more complex magnetic structures observed in neighboring  $\text{RMnO}_3$ , one may speculate that a similar complex structure could be induced in  $\text{GdMnO}_3$  for  $H||b$ , and this might explain the finite FE polarization via a coupling between AFM and FE order parameters.<sup>13,14</sup> Hence, there is need for a detailed determination of the magnetic structure of  $\text{GdMnO}_3$ .

In summary, we have presented a study of the magnetic-field temperature phase diagram of  $\text{GdMnO}_3$  via thermal expansion and magnetostriction measurements. We find that both, the ICAFM-to-cAFM as well as the FE transition are of first-order type and strongly hysteretic. The hysteresis is most pronounced in the low-field range. We find a down-bending of the ICAFM-to-cAFM phase boundary and evidence for coexisting ICAFM and cAFM phases in this low-field range.

The authors acknowledge fruitful discussions with D. Khomskii. This work was supported by the Deutsche Forschungsgemeinschaft through SFB 608. One of the authors (J.A.M.) is supported by the Alexander von Humboldt Stiftung.

\*Electronic address: lorenz@ph2.uni-koeln.de

- <sup>1</sup>T. Kimura, S. Ishihara, H. Shintani, T. Arima, K. Takahashi, K. Ishizaka, and Y. Tokura, *Nature (London)* **426**, 55 (2003).
- <sup>2</sup>T. Goto, T. Kimura, G. Lawes, A. P. Ramirez, and Y. Tokura, *Phys. Rev. Lett.* **92**, 257201 (2004).
- <sup>3</sup>M. Fiebig, T. Lottermoser, D. Frohlich, A. Goltsev, and R. Pisarev, *Nature (London)* **419**, 818 (2002).
- <sup>4</sup>T. Kimura, G. Lawes, T. Goto, Y. Tokura, and A. P. Ramirez, *Phys. Rev. B* **71**, 224425 (2005).
- <sup>5</sup>T. Kimura, S. Ishihara, H. Shintani, T. Arima, K. T. Takahashi, K. Ishizaka, and Y. Tokura, *Phys. Rev. B* **68**, 060403(R) (2003).
- <sup>6</sup>J. Hemberger, S. Lobina, H.-A. Krug von Nidda, N. Tristan, V. Y. Ivanov, A. A. Mukhin, A. M. Balbashov, and A. Loidl, *Phys. Rev. B* **70**, 024414 (2004).
- <sup>7</sup>T. Arima, T. Goto, Y. Yamasaki, S. Miyasaka, K. Ishii, M. Tsubota, T. Inami, Y. Murakami, and Y. Tokura, *Phys. Rev. B* **72**, 100102(R) (2005).

- <sup>8</sup>H. Kuwahara, K. Noda, J. Nagayama, and S. Nakamura, *Physica B* **359**, 1279 (2005).
- <sup>9</sup>K. Noda, S. Nakamura, J. Nagayama, and H. Kuwahara, *J. Appl. Phys.* **97**, 10C103 (2005).
- <sup>10</sup>According to T. Goto, Y. Yamasaki, H. Watanabe, T. Kimura, and Y. Tokura, *Phys. Rev. B* **72**, 220403(R) (2005), this discrepancy could also arise from weak oxygen off-stoichiometries in different crystals.
- <sup>11</sup>A. Kadomtseva, Y. Popov, G. Vorobév, K. Kamilov, A. Pyatakov, V. Ivanov, A. Mukhin, and A. Balbashov, *JETP Lett.* **81**, 19 (2005).
- <sup>12</sup>T. Lorenz, U. Ammerahl, T. Auweiler, B. Büchner, A. Revcolevschi, and G. Dhalenne, *Phys. Rev. B* **55**, 5914 (1997).
- <sup>13</sup>M. Mostovoy, *Phys. Rev. Lett.* **96**, 067601 (2006).
- <sup>14</sup>M. Kenzelmann, A. B. Harris, S. Jonas, C. Broholm, J. Schefer, S. B. Kim, C. L. Zhang, S.-W. Cheong, O. P. Vajk, and J. W. Lynn, *Phys. Rev. Lett.* **95**, 087206 (2005).